# Integration of the Compression Units of the Processing Plant with an Organic Rankin Cycle for Power Generation and Cooling Process

***Ali Allahyarzadeh Bidgoli[a], Jurandir Itizo Yanagihara[b]***

[a] *Department of Mechanical Engineering, Polytechnic School, University of São Paulo, São Paulo, Brazil, ali@usp.br*

[b] *Department of Mechanical Engineering, Polytechnic School, University of São Paulo, São Paulo, Brazil, jiy@usp.br,*

**Abstract:**

The gas compression units in the processing plant are used for various purposes. Compression of the associated gas is designed to adjust for the different operating pressures. In addition, the injection of $CO_2$ into oil reservoirs is used for enhanced oil recovery (EOR) and/or reduction of environmental impact. These systems utilize dozens of megawatts of electrical energy and intercooling for each compression stage. Therefore, the equipment used is energy-intensive and not thermodynamically efficient. An Organic Rankine Cycle (ORC) technology produces electrical energy from heat sources with low to medium temperature levels (90°C - 150°C). In the present work, a model of an ORC integrated with the intercoolers of the compression units is used to simulate the energy conversion of the system. Next, various working fluids, such as R123, n-butane, n-pentane, hexane, and n-heptane, are considered. The results show a possibility of net power generation by R123 ORC of up to 40 MW. Furthermore, only an increase of 0.95% in the $CO_2$ molar fraction of the flue gas leads to an increase of 1.29E8 kJ/h in the cooling demands of the $CO_2$ removal and compression units. Moreover, the presented increase in cooling demands creates the possibility of net power generation of up to 41 MW by ORC. Furthermore, in terms of footprint, this integrated system can be implemented in onshore structures and with some modifications in the condenser in offshore plants. Finally, this integrated system reduces environmental impacts by generating power from waste heat sources.

**Keywords:**

Multi-stage compression, Intercooling, Organic Rankine Cycle, Power production, Thermodynamic efficiency.

## 1. Introduction

Based on the IPCC Climate Change 2022 report, it is estimated that there will be a decrease of one billion tonnes of carbon dioxide emissions by 2050 [1]. Accordingly, decarbonization is no longer a prestige option in industries but is also an obligation for several industries, especially oil and gas industries with massive GHG emissions. In addition to the $CO_2$ removal unit of the oil and gas industries, the proper processing plant needs high cooling demands for the different cooling steps in gas compression units [2]. Attending to these demands and considering the environmental impacts is a dual challenge for the future of processing plants.

Typical processing plants consist of more than five gas compression steps to prepare the desired condition for exportation or injection [3, 4]. These steps need precooling, intercooling, and cooling to meet the required operating temperature. Therefore, the required cooling demands reach 100 MW for a typical processing plant [5, 6]. Conversely, due to the high operating pressure and temperature of the gas compression unit, the equipment used is energy-intensive and is not thermodynamically efficient [7].

An Organic Rankine Cycle (ORC) system is a thermodynamic process utilized for small to medium-scale implementations in several operating temperature ranges and electricity productions using small to intermediate and high-temperature heat supplies varying from 80 to 400°C. With the help of a closed cycle, the limited heat that might otherwise be wasted can be used effectively [8, 9] for power generation. This technology can also mitigate environmental impacts by managing and using waste heating sources [10].

Vilarini et al. [8] and Morais et al. [11] show that the selection of an organic fluid for a system depends on the evaporation enthalpy, dry, isentropic (or wet) characterization, and the slope of the saturation vapor curve of the T-s diagram of the working fluid. In addition to traditional hydrocarbons as working fluids of ORC, such as

https://doi.org/10.52202/069564-0132

n-butane, heptane, propane, etc, the refrigerants of the R12XX family present outstanding performance [12, 13] for certain operating conditions. This positive effect on thermodynamic performance is more prominent when applying regenerative ORC [12].

To the author's knowledge, no other research group evaluated the performance of different working fluids for the cooling process of an ORC that uses the waste heat of compression units of a typical processing plant as the heating source. Moreover, the impact of the $CO_2$ molar fraction in the flue gas on the cooling demand of a processing plant and the analysis of using this waste heating for power production by ORC is not presented in the open literature.

Therefore, to fill the existing gaps and evaluate possible solutions, a model of an ORC integrated with the intercoolers of the compression units is used to simulate the energy conversion of the system. Next, various working fluids, such as R123, n-butane, n-pentane, hexane, and n-heptane, are considered. In addition, the impact of the variation of the $CO_2$ molar fraction in the process stream is investigated, and its effect on the cooling demands of the compression unit and the power generated for each working fluid is calculated. Finally, the dimensions of the installation for application in onshore and offshore structures and the environmental impacts of this integration are discussed.

# 2. Process Simulator and Problem Setup

## 2.1. System description

### 2.1.1 Compression units

As Figure 1 shows, the organic Rankin cycle uses the waste heating of the following unit to meet cooling and power generation demands:

1- **Main gas compression**
This unit is responsible for compressing the associated gas of the fluid reservoirs, including $CO_2$ and natural gas components, for the following processing units at operating pressures of up to 8500 kPa. The suction pressure of compression is 2000 kPa. This unit has precooling and cooling heat exchangers [3].

2- **Vapor recovery unit**
The vapor recovery unit increases and adjusts the operating pressure of the separated gas in different steps of the separation train and the suction temperature of the main gas compressor. This unit comprises two compressor stages with two operating conditions and cooling heat exchangers [14].

3- **Exportation Gas Compression**
The exportation gas system receives gas with the suction pressure of the compressors at 250 bar. Note that the cooling steps of the compression system provide heating sources for a Rankine cycle for power generation [15].

4- **$CO_2$ compression**
The gases separated in membrane $CO_2$ separators from the fluid reservoir and the $CO_2$ captured by the MEA solution-based mechanism from the combustion product are prepared in these systems. The discharge pressure of these units can reach up to 25 MPa. These units comprise four compression stages and the corresponding intercoolers [7].

5- **Carbon capture**
The carbon capture unit or the $CO_2$ removal unit presents a huge cooling demand for the condenser of the stripper tower, which is a significant source of waste heat for use in the organic Rankine cycle [5].

Table 1 shows the operating conditions of the compression unit of a typical processing plant (offshore and FPSO) that works with many gas and $CO_2$ in reservoir fluid.


https://doi.org/10.52202/069564-0132

**Table 1.** Specification of gas compression units [16].

| Main unit | Description | Value |
| --- | --- | --- |
| **Gas treatment** | Number of the main units | 5 |
| Vapor recovery | Operating pressure of suction-discharge (kPa) | 770–2000 |
| Main compression | Operating pressure of suction-discharge (kPa) | 2000 –8500 |
| | Compression capacity ($Sm^3/d$) | 6,000,000 |
| | Number of stages | 2 |
| Gas exportation | Operating pressure of suction-discharge (kPa) | 4500–25,000 |
| | Compression capacity ($Sm^3/d$) | 3,000,000 |
| **$CO_2$ treatment** | Number of main units | 3 |
| | Number of stages | 4 |
| $CO_2$ compression | Operating pressure of suction-discharge (kPa) | 400–25,000 |

As shown in Figure 1, the heat transferred from three systems is the heat source for the organic Rankine cycle. In fact, in each unit, there are a number of heat exchangers (pre-coolers, intercoolers, and coolers) connected to the ORC system. From the point of view of the ORC system, the heating is absorbed in three stages: economizer, evaporator, and superheater. Furthermore, the ORC uses a regenerative heat exchanger to increase energy efficiency.

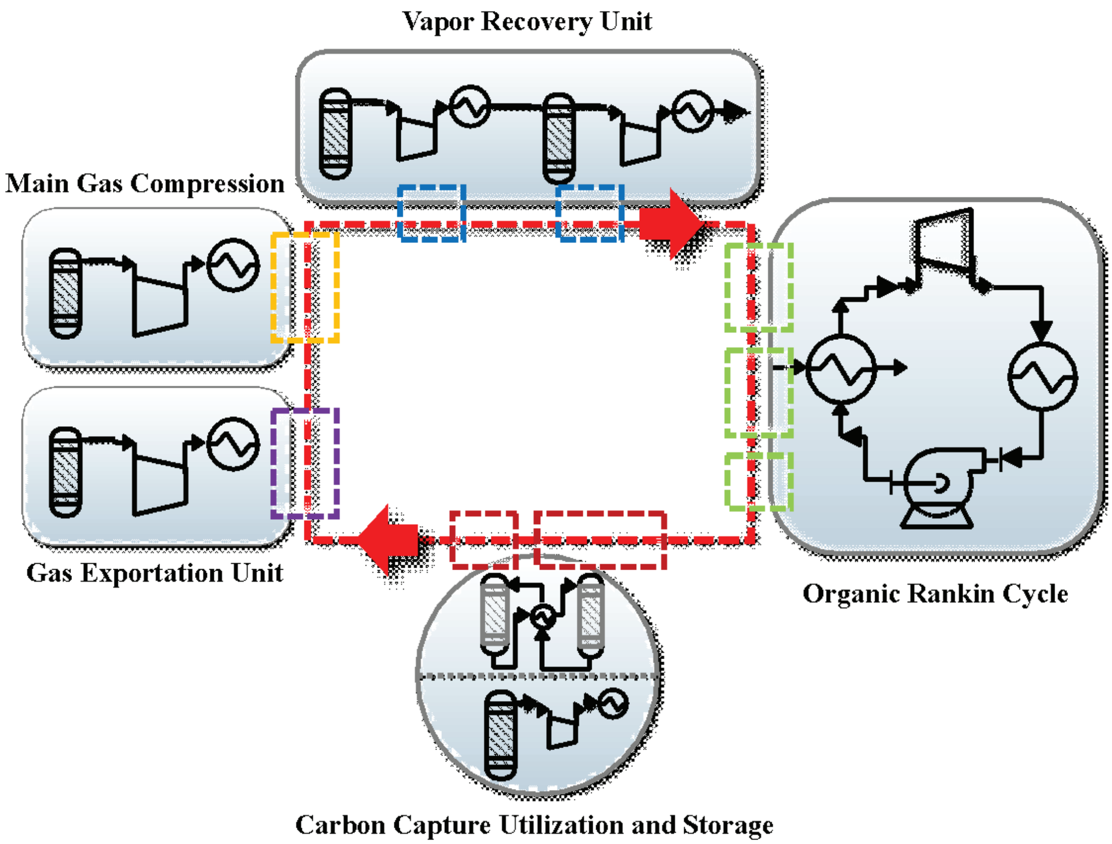


**Figure 1**. A Conceptual flow diagram of compression units and Organic Rankin Cycle

### 2.1.2 Organic Rankin Cycle

In this study, as previously mentioned, a regenerative ORC is simulated. To evaluate the performance of different working fluids with respect to the operating condition of the cooling heat exchangers, four distinct fluids with different thermodynamic properties are implemented, as seen in Table 2. In this case, n-butane presents the minimum boiling point and critical temperature, while the lowest critical pressure belongs to n-heptane. After R123, the next lowest critical temperature is for n-hexane. Figure 2 presents the temperature vs. entropy diagrams calculated for n-pentane in this study. Figure 2 also shows the quality lines, different pressure lines, and connected saturate states.

**Table 2**. Boiling point, critical temperature, and critical pressure of applied working fluids

| Fluid | Boiling Point (°C) | Critical Temperature (°C) | Critical Pressure (kPa) |
|---|---|---|---|
| n-pentane | 36.06 | 196 | 3367 |
| n-butane | -0.50 | 152 | 3797 |
| n-hexane | 68.73 | 234.7 | 3032 |
| n-heptane | 98.4 | 267 | 2736 |
| R123 | 27.8 | 183.6 | 3661 |


https://doi.org/10.52202/069564-0132

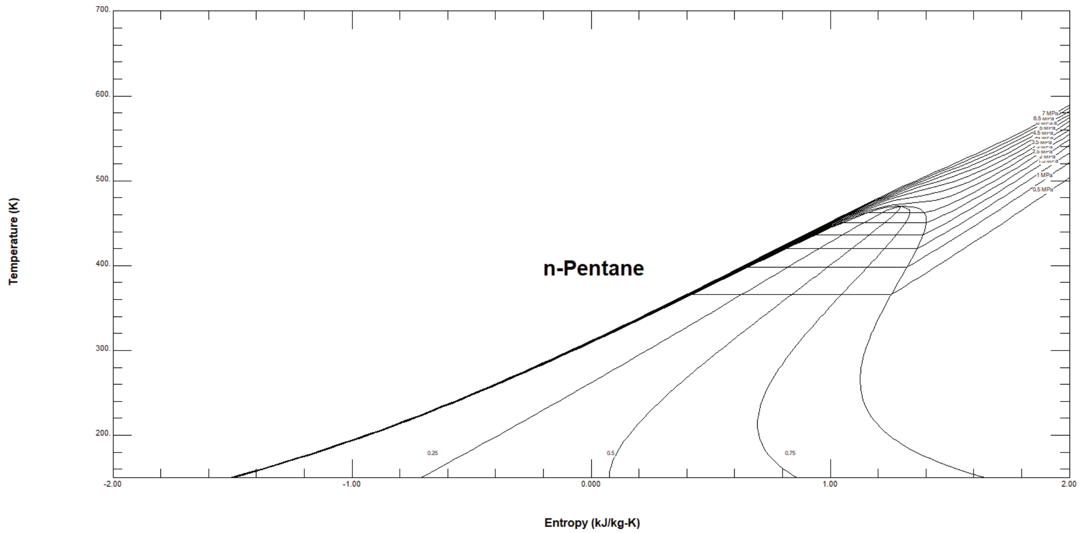


**Figure 2**. T-s diagram of the applied working fluid (n-pentane)

### 2.2 Assumptions and numerical modeling

The following assumptions are considered or adopted for numerical simulations:

- The environmental pressure is considered to be 101 kPa, and the ambient temperature is 25 $^{o}$C [11].
- A polytropic efficiency of 85% is considered for all centrifugal compressors [7];
- The isentropic efficiency of the steam turbine is considered to be 90% [11];
- Aspen HYSYS [17] is used for model development. Due to the different operating pressures, temperatures, and compositions of each unit, a multi-EoS simulation (PR [18], Span-Wagner [19], and Acid Gas [20]) is considered for the calculation of thermodynamic properties;
- Heat loss and fluid leakage are considered negligible for the heat exchangers.
- The pressure drop of pre-coolers, intercoolers, and coolers is adjusted for 50 kPa based on technical documents, and the pressure drop in other heat exchangers is negligible [16];
- To avoid the temperature cross in the heat exchangers, the minimum temperature approach is set at 2 $^{o}$C [3].

## 3. Methodologies

### 3.1. Thermodynamic analysis process

Equations 1 and 2 are the mass and energy balances for volume control in a steady state

$$\sum \dot{m}_{in} - \sum \dot{m}_{out} = 0 \tag{1}$$

$$\dot{Q} - \dot{W} + \sum \dot{m}_{in} h_{in} - \sum \dot{m}_{out} h_{out} = 0 \tag{2}$$

where $\dot{m}$ = mass flow rate
$\dot{Q}$ = heat generated or rejected
$\dot{W}$ = work consumed or produced
h = specific enthalpy

*in* and *out*= input and output.

The total heat transferred between the tube and shell sides (Heat Exchanger duty) can be defined in terms of the overall heat transfer coefficient, the area available for heat exchange, and the log mean temperature difference as Equation 3 presents

$$Q = UA\Delta T_{LM} F_t \tag{3}$$

where

U = overall heat transfer coefficient

A = surface area available for heat transfer

$\Delta T_{LM}$ = logarithmic mean temperature difference (LMTD)

$F_t$ = LMTD correction factor

The following general relation applies to the shell side of the heat exchanger.

$$m_{shell}(h_{in} - h_{out})_{shell} - Q_{loss} + Q = \rho \frac{d(Vh_{out})_{shell}}{dt} \tag{4}$$

For the tube side

$$m_{tube}(h_{in} - h_{out})_{tube} + Q = \rho \frac{d(Vh_{out})_{tube}}{dt} \tag{5}$$

where:

$m_{shell}$ = shell fluid flow rate

$m_{tube}$ = tube fluid flow rate

$\rho$ = specific mass

h = enthalpy

$Q_{loss}$ = heat loss

Q = heat transfer from the tube side to the shell side

V = volume of shell or tube holdup

## 4. Results

This section presents and discusses the results of the integration of the compression unit with ORC. First, the calculated duty of each unit's heat exchangers that can be used as the heat source for the ORC is presented. Then, the power generated and applied operating conditions for the ORC are shown. In addition, the variation of the $CO_2$ molar faction in the process stream is discussed, and finally, a discussion regarding weight and footprint is presented.

## 4.1 Waste heat of compression units

Hydrocarbon fluid can be extracted directly from the processing plant for use as the working fluid in the ORC. As the operating conditions of precooling, intercooling, and condensers are different**,** it is essential to adjust the heat exchanger for feasible and acceptable heat transfer. For example, avoiding temperature cross is an important matter for using the waste heat of the compression unit in the ORC.

Figure 3 shows the waste heat available for recovery in the compression and $CO_2$ removal units. In that, a MEA-based solution to separate $CO_2$ presents a cooling demand of approximately 1.4 X 10 $^{8}$ kJ/h that can be used for ORC. Figure 3 shows that this waste heat is more than 37% of the total heating source, being the highest. Next, the heat exchangers for precooling, intercooling, and cooling of the $CO_2$ compression unit, the exportation gas compression, the main gas compression, and the vapor recovery unit represent, respectively, 23.5%, 23.1%, 13.7 %, and 2.4% of waste heat recovery, as can be seen in Figure 3.


https://doi.org/10.52202/069564-0132

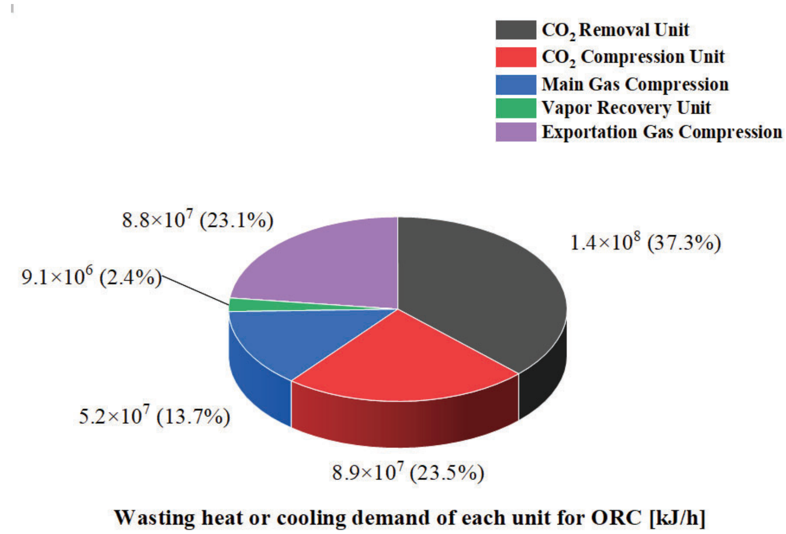


**Figure 3.** Existing duty of the applied heat exchanger for using the waste heat of coolers as the heat source of the ORC

Figure 4 shows the power generated by the different working fluids in Table 2. The performance of N-pentane, n-butane, hexane, n-heptane, and R123 is evaluated and presented in Figure 4. Figure 4 shows that R123 yields a power of 41 MW, and n-hexane achieves a power generation of 34.7 MW, which is more than 32% of the total power demand of a typical offshore structure [3, 15]. After n-hexane, n-pentane presents a power generation close to 32 MW and is in third place in terms of power generation. Furthermore, as shown in Figure 4, n-butane and n-heptane present a power generation of 18.6 and 27.8 MW, respectively. As can be seen here, R123 presents the highest power generated for the present operating conditions and the existing waste heat of a typical processing plant.

Figure 5 presents the work consumed by the pumps of ORCs. In that, an ORC with R123 as the working fluid needs a pump that consumes 973 kW of electrical energy. Next, the shaft work of pumps of the ORC working with n-pentane, n-butane, n-hexane, and n-heptane are 546, 375, 318, and 147 kW, respectively.

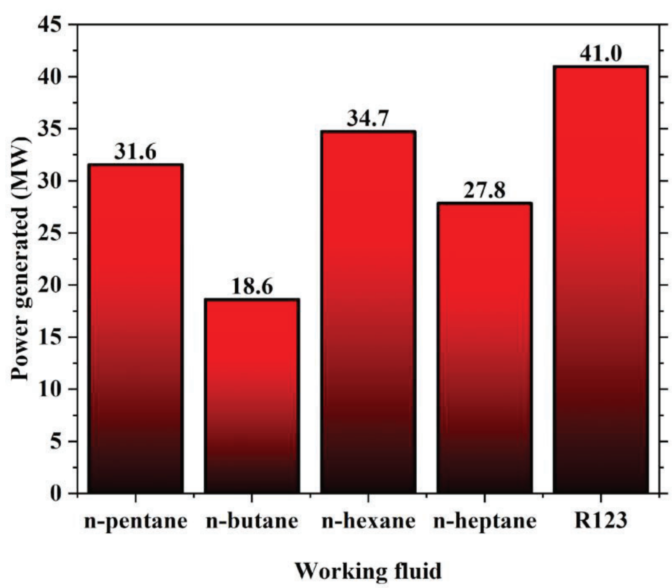


**Figure 4.** Power generated by working fluid applied in a typical processing plant of this study

https://doi.org/10.52202/069564-0132

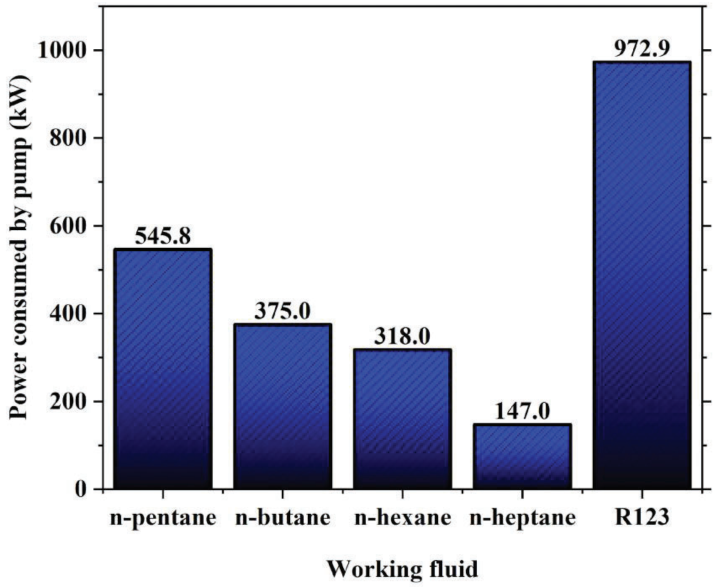


**Figure 5**. Power consumed by pumps of ORC working fluid applied in a typical processing plant of this study

Table 3 shows the operating condition of R123 ORC with the maximum power generated compared to other fluids. Based on that, the outlet temperature of the cold fluid from the regenerator is 36 $^{o}$C, and the inlet temperature of the steam turbine is 123.3 $^{o}$C, as can be observed in Table 3. The cooling demands of 10 heat exchangers from different units are used as the heat sources for the ORC. Table 3 shows that this arrangement generates 40 MW of power.

**Table 3.** Specification of R123 ORC

| Section | Description | value |
|---|---|---|
| Organic Rankin Cycle | Operating fluid | R123 |
| | Type of ORC | Regenerative |
| | Outlet temperature of cold fluid from the regenerator | 36 $^{o}$C |
| | Inlet temperature of steam turbine | 123.3 $^{o}$C |
| | Type of heating sources | Precooling, intercooling and cooling shell and tube HE |
| | Number of heating sources | 10 |
| | Net Power generation | 40 MW |
| | Overall required power | 973 kPa |

### 4.2 Sensitivity analysis of $CO_2$ molar fraction on the power generation and heating sources of compression units

Figure 6 shows the effect of the $CO_2$ molar fraction of the flue gas on the power generation of the applied working fluids. In this case, $CO_2$ molar fractions of 2.65%, 3.1%, and 3.6% in the flue gas input mass flow rate are evaluated. This flue gas enters the $CO_2$ removal units, and then the separated $CO_2$ is sent to storage or utilization purposes. Note that as the mass flow rate increases, the required cooling demands increase for the condenser in the stripper tower of the $CO_2$ removal unit and the intercoolers of the $CO_2$ compression unit.

The increase in the heat provided to the ORC results in a higher temperature of the working fluid in the input of the steam turbine and ends with more power generated, as can be observed in Figure 6. In detail, with an


https://doi.org/10.52202/069564-0132

increase of 0.95% in the $CO_2$ molar fraction of flue gas, the power generated by R123 can increase to approximately 2% (41.81 MW), as can be seen in Figure 6. Moreover, Figure 6 presents the increase in $CO_2$ processing from the baseline of 2.63% to 3.6%, leading to an increase in the power generated by n-butane ORC of up to 20 MW (an increase of 1.45 MW).

Figure 7 introduces the effect of the $CO_2$ molar fraction of the flue gas on the waste heat of $CO_2$ processing plants, such as the $CO_2$ removal unit and the $CO_2$ compression unit. With a 0.02% increase in the $CO_2$ molar fraction of the flue gas, the cooling demand of the plants increases from 7.99E8 kJ/h to 8.28E8 kJ/h, as shown in Figure 7. Moreover, Figure 7 shows that an increase of 0.95% in the $CO_2$ molar fraction results in a waste heat of 9.19E9 kJ/h, which presents an increase of 15% (1.29E8 kJ/h).

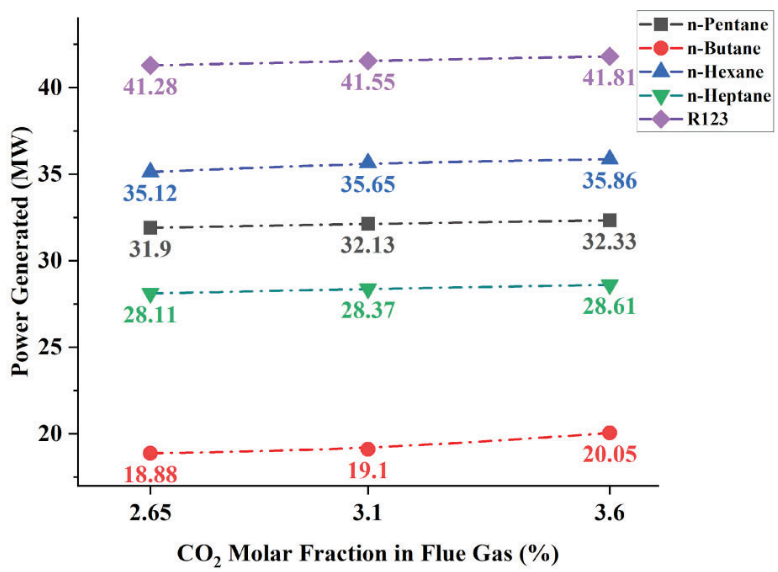


**Figure 6.** The effect of the $CO_2$ molar fraction of the flue gas on the power generation of working fluids.

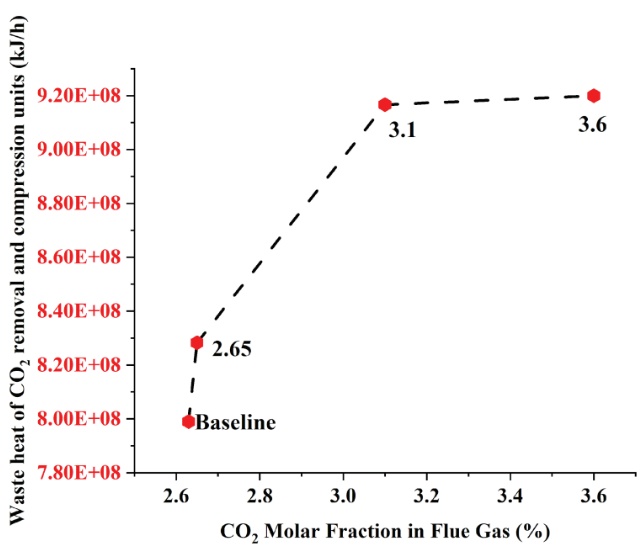


**Figure 7.** The effect of $CO_2$ molar fraction of flue gas on the waste heat of regarding processing plant to $CO_2$.

### 4.3 Footprint analysis of the proposed Organic Rankin Cycle

As a novelty of this work, there is no research in the open literature focused on the integration of compression units with an ORC for power generation and process cooling in an offshore processing plant. For such applications, the footprint and weight of any added system are crucial because they may imply a complete redesign of the whole haul [21].

For onshore applications, we present the following information. In terms of required footprint, based on the commercial data of an existing ORC system (without indicating the working fluid), for a geothermal heating source with an inlet steam temperature of 130 $^oC$, a footprint for two 22.5 MW ORCs is approximately 30,000 $m^2$ [22]. These plants use radial outflow turbines that can work with two operating pressures.

As the satellite figures show (Figure 8, a and b), more than half the occupied footprint of these plants belongs to the air coolers of the condenser. In ORC integrated systems in processing plants, these air coolers can be replaced by shell and tube heat exchangers to meet the cooling demand, with a much smaller footprint. Although further studies focused on the topsides configuration are needed for offshore applications, the potential of this system for energy saving was clearly demonstrated.

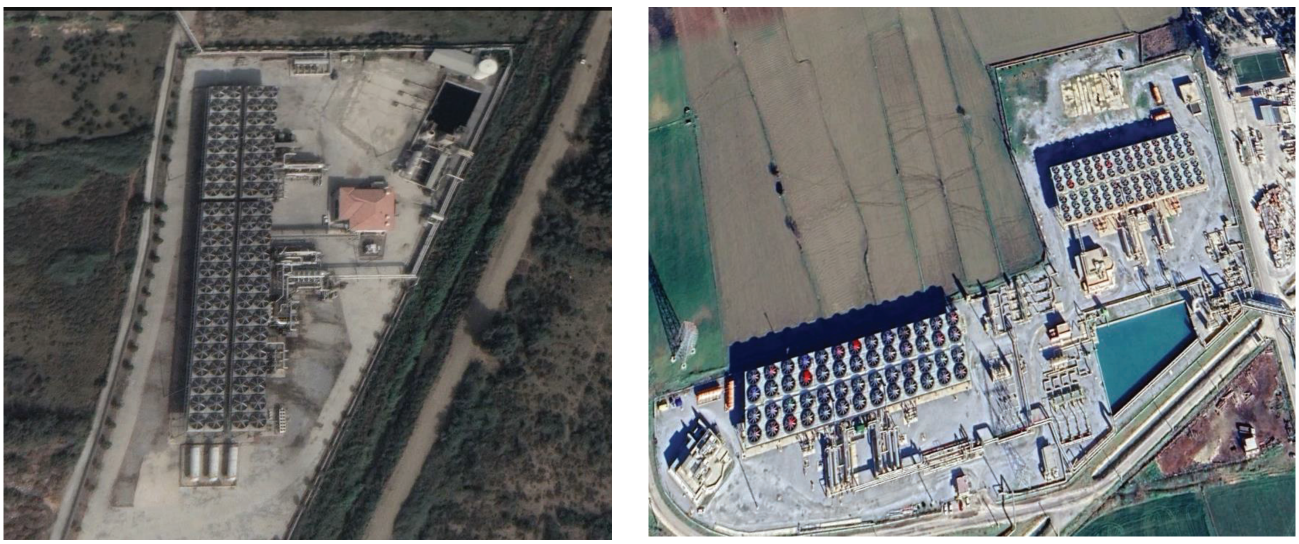

(a) (b)

**Figure 8.** ORC plants of up to 50 MW with geothermal heat sources: a) one of 22.5 MW, of two (Ken Kipaş), b) two of 24 MW (Kubilay I, II)

## 5. Conclusions

In this research, a model of an ORC integrated with the intercoolers of the compression units was used to simulate the energy conversion of the system. Next, various working fluids, such as R123, n-butane, n-pentane, hexane, and n-heptane, were applied for ORC to evaluate the most efficient with respect to power generation. Then, the variation of the $CO_2$ molar fraction in the flue gas was analyzed, and its effect on the cooling demands of the compression unit and the power generated for each working fluid was presented.

Integration was carried out successfully with ten heat exchangers, and R123 obtained up to 40 MW of net power generation. In addition, an increase of 0.95% in the $CO_2$ molar fraction of flue gas resulted in an increase of 15% in cooling demands of the units for $CO_2$ processing and the possibility of power generation of 41.81 MW by R123 ORC.

Regarding the required footprint for the presented ORC, it may be feasible to use it in onshore structures. Moreover, an offshore application can be made by redesigning the air cooler for the ORC condenser to use this heat source.

Furthermore, the presented system significantly decreases the environmental impact, namely the global warming effect of the compression units, because the cooling demands can be addressed by atmospheric air or seawater. On the other hand, any increase in the capacity of the $CO_2$ removal unit and its increase in cooling demands can be managed and converted to power generation. Finally, this system can be implemented for several industries with large gas compression units, and the recovered heat can be used to generate power.

 https://doi.org/10.52202/069564-0132

## Acknowledgments

Jurandir Itizo Yanagihara would like to acknowledge CNPq (National Council for Scientific and Technological Development - Brazil) for the research grant 306364/2020-4.

## Nomenclature

| | |
|---|---|
| A | Surface area available for heat transfer ($m^2$) |
| $F_t$ | LMTD correction factor |
| FPSO | Floating Production Storage and Offloading |
| $h$ | Specific enthalpy (kJ/kg) |
| $\dot{m}$ | Mass flow rate (kg/s) |
| MEA | Monoethanolamine |
| PR | Peng-Robinson |
| $\dot{Q}$ | Heat rate (kW) |
| T | Temperature (°C) |
| U | Overall heat transfer coefficient (W/($m^2$.K)) |
| $V$ | Volume, ($m^3$) |
| $\dot{W}$ | Work, (kW) |

**Greek symbols**

| | |
|---|---|
| $\rho$ | Specific mass (kg/$m^3$) |
| $\Delta T_{LM}$ | Log mean temperature difference (LMTD) |

**Subscripts and superscripts**

| | |
|---|---|
| $in$ | input |
| $out$ | output |

## References

[1] Pörtner, H.-O., et al., IPCC, 2022: Summary for policymakers. 2022.

[2] Allahyarzadeh Bidgoli, A., N. Hamidishad, and J.I. Yanagihara, The impact of carbon capture storage and utilization on energy efficiency, sustainability, and production of an offshore platform: thermodynamic and sensitivity analyses. Journal of Energy Resources Technology, 2022. **144**(11): p. 112102.

[3] Bidgoli, A.A., Simulation and optimization of primary oil and gas processing plant of FPSO operating in pre-salt oil field. 2018, Universidade de São Paulo.

[4] Nguyen, T.-V., et al., A novel methodology for the design and optimisation of oil and gas offshore platforms. Energy, 2019. **185**: p. 158-175.

[5] Allahyarzadeh-Bidgoli, A., N. Hamidishad, and J.I. Yanagihara, Carbon capture and storage energy consumption and performance optimization using metamodels and response surface methodology. Journal of Energy Resources Technology, 2022. **144**(5).

[6] Hunt, J.D., et al., Deep seawater cooling and desalination: Combining seawater air conditioning and desalination. Sustainable Cities and Society, 2021. **74**: p. 103257.

[7] Allahyarzadeh-Bidgoli, A., et al., Thermodynamic analysis and optimization of a multi-stage compression system for CO 2 injection unit: NSGA-II and gradient-based methods. Journal of the Brazilian Society of Mechanical Sciences and Engineering, 2021. **43**: p. 1-19.

[8] Villarini, M., et al., Influence of the incident radiation on the energy performance of two small-scale solar Organic Rankine Cycle trigenerative systems: A simulation analysis. Applied Energy, 2019. **242**: p. 1176-1188.

[9] Ahmadi, A., et al., Applications of geothermal organic Rankine Cycle for electricity production. Journal of Cleaner Production, 2020. **274**: p. 122950.

[10] Imran, M., et al., Optimization of organic rankine cycle power systems for waste heat recovery on heavy-duty vehicles considering the performance, cost, mass and volume of the system. Energy, 2019. **180**: p. 229-241.
[11] da Silva Morais, P.H., et al., Energy, exergetic and economic analyses of a combined solar-biomass-ORC cooling cogeneration systems for a Brazilian small plant. Renewable Energy, 2020. **157**: p. 1131-1147.
[12] Zhar, R., et al., A comparative study and sensitivity analysis of different ORC configurations for waste heat recovery. Case Studies in Thermal Engineering, 2021. **28**: p. 101608.
[13] Ata, S., A. Kahraman, and R. Şahin, Prediction and sensitivity analysis under different performance indices of R1234ze ORC with Taguchi's multi-objective optimization. Case Studies in Thermal Engineering, 2020. **22**: p. 100785.
[14] Allahyarzadeh-Bidgoli, A., et al., Energy optimization of an FPSO operating in the Brazilian Pre-salt region. Energy, 2018. **164**: p. 390-399.
[15] Allahyarzadeh-Bidgoli, A., et al., FPSO fuel consumption and hydrocarbon liquids recovery optimization over the lifetime of a deep-water oil field. Energy, 2019. **181**: p. 927-942.
[16] Allahyarzadeh-Bidgoli, A. and J.I. Yanagihara, Energy efficiency, sustainability, and operating cost optimization of an FPSO with CCUS: An innovation in CO2 compression and injection systems. Energy, 2023. **267**: p. 126493.
[17] Aspen HYSYS 2017, Aspen Technology Inc. .
[18] Peng DY, R.D., A new two-constant equation of state. . Ind Eng Chem Res, 1976. **15**: p. 59-64.
[19] Span R, W.W., A new equation of state for carbon dioxide covering the fluid region from the triple-point temperature to 1100 K at pressures up to 800 MPa. J Phys Chem Ref Data, 1996. **25**(61): p. 509–9.
[20] Austgen DM, R.G., Peng X, Chen CC., Model of vapor-liquid equilibria for aqueous acid gas-alkanolamine systems using the electrolyte-NRTL equation. Ind Eng Chem Res, 1989. **28**(7): p. 1060–73.
[21] Pereira, L.A.G., J.I. Yanagihara, Sensitivity analysis and optimization to reduce dry weight and footprint of FPSO processing plants in a high CO2 oil field. Comp & Chemical Eng, 2022. **156**: p. 107576.
[22] SRL, E.I. GREENECO ENERJI. [cited 2023; Available from: https://www.exergy-orc.com/casi-studio/greeneco-enerji/.

 https://doi.org/10.52202/069564-0132